Phase Space Features and Statistical Aspects of Forward−Backward Semiclassical Dynamics†

Nicholas J. Wright and Nancy Makri*

Department of Chemistry, University of Illinois, 601 South Goodwin Avenue, Urbana, Illinois 61801

Received: November 25, 2003; In Final Form: January 29, 2004

Forward−backward semiclassical dynamics (FBSD) has emerged as a practical quasiclassical methodology for including important quantum mechanical effects in the initial state of a system, while retaining a classical description of the subsequent dynamics. FBSD expressions for time correlation functions or expectation values constitute rigorous stationary phase limits of the corresponding quantum mechanical quantities but can be evaluated with relatively little computational power. While allowing the inclusion of important effects such as zero point energy, the mixing of a quantum mechanical representation of the initial condition with a classical treatment of the dynamics is at least in principle inconsistent. In this paper we investigate various manifestations of this issue. Specifically, we examine the classical evolution of the quantized FBSD phase space density and the validity of the detailed balance condition in model systems. Our findings indicate that the practical consequences of the inconsistent quantum-classical treatment generally are of minor significance and suggest specific tests for checking the accuracy of FBSD calculations in polyatomic systems.

I. Introduction

In recent years there has been renewed interest in the use of time-dependent semiclassical theory[1,2] as a practical way of including quantum mechanical effects into classical molecular dynamics simulations.[3−58] The semiclassical approximation provides an attractive method because it is based on classical trajectories, allowing one to obtain an intuitive understanding of the dynamical process being investigated, as well as taking advantage of the efficient and well-developed molecular dynamics technology.

The use of semiclassical methods has, however, been plagued by some serious difficulties. Perhaps the most severe of these is the so-called "sign problem" that arises from the rapidly oscillatory semiclassical phase. A practical way to sidestep this problem and allow the calculation of correlation functions for complex systems, albeit with the loss of some quantum mechanical information, is the use forward−backward semiclassical methods.[25−30,32,33,36−40,42,57,58] The basic idea of forward−backward semiclassical dynamics (FBSD) is to combine the two time evolution operators present in the expression for the correlation function into *a single* semiclassical propagator, which is equivalent to an additional stationary phase approximation in all (or just some) of the degrees of freedom involved. This approximation reduces the oscillatory character of the integral substantiality at the expense of eliminating (at least partially) quantum interference effects. In condensed phase systems the effects of such interference are usually insignificant because of extensive decoherence. In such cases the forward−backward semiclassical approximation is both well-justified and accurate.

Recent work in our group has concentrated on a quasiclassical expression for the correlation function, derived from a particular formulation of FBSD developed in our group.[29,30,59] By combining this with a fully quantum mechanical imaginary time path integral description of the density operator, a methodology has been developed for the calculation of correlation functions at finite temperature.[37,57,58,60]

In this paper we examine some properties of quasiclassical FBSD correlation functions employing a quantized initial density. We study the behavior of the quantized phase space distribution under classical evolution and the consequences of the apparent violation of stationarity caused by the classical propagation of this function. We also investigate the validity of detailed balance relations that connect the real and imaginary parts of a time correlation function and identify sensitive tests for assessing the accuracy of FBSD calculations in many-particle systems. Finally, we comment on optimal choices of the coherent state parameter that enters FBSD expressions.

Section II reviews the theoretical framework of FBSD for time correlation functions. Section III discusses theoretical issues associated with the use of classical mechanics to propagate a quantized density. The question of detailed balance preservation is introduced in section IV. In section V we address the above issues by analyzing limiting cases and presenting numerical calculations on a strongly anharmonic one-dimensional oscillator. Section VI discusses practical considerations related to the optimal choice of the coherent state parameter and to devising tests for checking the convergence and accuracy of the FBSD results. Finally, section VII presents some concluding remarks.

II. Review of Forward−Backward Semiclassical Dynamics

The goal of semiclassical methods is to yield reasonably accurate approximations to time-dependent observables (or functions that are related to observables). Our emphasis in the present paper is on expectation values or time correlation functions of the type

$$C_{AB}(t) = \mathrm{Tr}(\hat{\rho}_0 \hat{A} e^{i\hat{H}t/\hbar} \hat{B} e^{-i\hat{H}t/\hbar}) \qquad (2.1)$$

† Part of the special issue "Hans C. Andersen Festschrift".
* Corresponding author.

10.1021/jp037600f CCC: $27.50
Published on Web 03/25/2004

where $\hat{H}$ is the Hamiltonian operator and the density operator $\hat{\rho}_0$ specifies the initial condition. For simplicity we use one-dimensional notation throughout this article. The multidimensional versions of the FBSD expressions have been given in other publications by our group.[57,58,60]

The full semiclassical representation of eq 2.1 is obtained by expressing each of the forward and reverse time evolution operators by their semiclassical approximation. The most convenient representation in terms of coherent states takes the form[5]

$$e^{-i\hat{H}t/\hbar} = (2\pi\hbar)^{-1}\int \mathrm{d}x_0 \int \mathrm{d}p_0 |g_{x_t,p_t}\rangle D(x_0, p_0)\, e^{iS(x_0,p_0)/\hbar}\langle g_{x_0,p_0}| \quad (2.2)$$

Here x_t, p_t are the phase space coordinates of a trajectory originating at x_0, p_0, S is the corresponding classical action, D is an appropriate prefactor that depends on the stability characteristics of the trajectory, and g_{x_0,p_0} are coherent states described by complex-valued Gaussians

$$\langle x|g_{x_0p_0}\rangle = \left(\frac{2}{\pi}\right)^{3/4}\gamma^{1/4}\exp\left[-\gamma(x-x_0)^2 + \frac{i}{\hbar}p_0(x-x_0)\right] \quad (2.3)$$

which are centered in phase space about the coordinates x_0, p_0. As is well-known, the semiclassical phase in eq 2.2 oscillates rapidly, and this behavior causes severe problems for Monte Carlo integration methods.

The basic idea of the forward−backward formulation is to combine the time evolution operator and its adjoint in eq 2.1 into a *single* semiclassical propagator that describes the evolution of the system to time t and back again to zero time. This can be achieved if one is able to take account of the effect of the $\hat{B}$ operator at the end of the forward evolution part. To date, two exponential representations of $\hat{B}$ have been used: the Fourier method of Miller and co-workers[26,32] and the derivative formulation developed by Shao and Makri.[29,30] Thoss et al.[40] have developed a generalized forward−backward methodology, which interpolates continuously between the full (double phase space integral) semiclassical result and its forward−backward (stationary phase) limit. The presence of an oscillatory factor in these methods generally makes computation more demanding, but Yamamoto et al.[54] have recently shown that application to a particular symmetric form of the flux correlation function (whose integral yields the rate constant of a bimolecular reaction), along with appropriate stationary phase filtering,[50] can sufficiently smooth the integrand, allowing calculations in systems with more than 100 degrees of freedom. The derivative formulation[29,30] and also an approximate (linearized) version of the full semiclassical expression[61] lead to appealing *quasi-classical* expressions that are free of the rapidly oscillating semiclassical phase. (Note, however, that the slowly varying phase of the coherent state functions remains in the derivative FBSD expression, eq 2.10 below; this phase is important for certain quantum features of the dynamics.)

In this work we use the derivative FBSD formulation,[29,30,59] which makes use of the identity

$$\hat{B} = -i\frac{\partial}{\partial\mu}e^{i\mu\hat{B}}|_{\mu=0} \quad (2.4)$$

to bring the second operator into an exponential form. Thus, the time-dependent part of the correlation function is represented by three consecutive exponentials, and the Heisenberg form of $\hat{B}$ is expressed as

$$\hat{B}(t) \equiv e^{i\hat{H}t/\hbar}e^{i\mu\hat{B}}e^{-i\hat{H}t/\hbar} = -i\frac{\partial}{\partial\mu}e^{i\hat{H}t/\hbar}e^{i\mu\hat{B}}e^{-i\hat{H}t/\hbar}|_{\mu=0} \quad (2.5)$$

The derivation of the derivative-FBSD expression has been described in detail in previous publications[29,30,37,38,60] and we only give a brief summary here.

After inserting eq 2.5 into eq 2.1 and using the coherent state representation of the semiclassical propagator[5] on the product of the three exponential operators, eq 2.2, the Heisenberg form of $\hat{B}$, becomes[29,30,38,59]

$$\hat{B}(t) = -i(2\pi\hbar)^{-1}\frac{\partial}{\partial\mu}\int \mathrm{d}x_0 \int \mathrm{d}p_0 \exp\left(\frac{i}{\hbar}S_f(x_0, p_0)\right)|g(x_f, p_f)\rangle \langle g(x_0, p_0)|\Big|_{\mu=0} \quad (2.6)$$

Here the phase space variables x_0, p_0 specify initial conditions for classical trajectories, which are first integrated forward to the time t. At that time the trajectories incur position and momentum jumps given by the relations

$$\delta x_t = -\frac{1}{2}\hbar\mu\frac{\partial}{\partial p_t}B(x_t, p_t)$$

$$\delta p_t = \frac{1}{2}\hbar\mu\frac{\partial}{\partial x_t}B(x_t, p_t) \quad (2.7)$$

while the action increments by the amount

$$\delta S_t = \hbar\mu B(x_t, p_t) + p_t\delta x_t \quad (2.8)$$

Subsequently, each trajectory is integrated back to time zero following the classical equations of motion, reaching the phase space point x_f, p_f, and the total accumulated action has the value S_f.

The notable feature of eq 2.6 is the absence of the semiclassical prefactor. Elimination of the latter has been achieved by linearizing the final trajectory values and the action in the infinitesimal parameter μ and rescaling the position and momentum jumps to compensate for the prefactor. For this reason the trajectory increments given in eq 2.7 are equal to *one-half* of the values dictated by the classical equations of motion that correspond to the product of exponential operators in eq 2.5.[29,30]

The infinitesimal character of the trajectory jumps at the end of the forward propagation implies that the cross terms between distinct forward and backward trajectories have been neglected. Thus, eq 2.6 cannot account for quantum interference effects. As stated in the Introduction, such effects are strongly quenched in systems of many degrees of freedom. Because of this natural decoherence, FBSD can provide an accurate approximation to condensed phase dynamics.

The above structure also allows transformation of eq 2.6 to a derivative-free form that involves trajectories only in the forward time direction.[40,59] Thus, the Heisenberg operator takes the form

$$\hat{B}(t) = (2\pi\hbar)^{-1}\int \mathrm{d}x_0 \int \mathrm{d}p_0\, B(x_t, p_t) \times \left(\frac{3}{2}\Big|g_{x_0,p_0}\rangle\langle g_{x_0,p_0}| - 2\gamma(\hat{x}-x_0)|g_{x_0,p_0}\rangle\langle g_{x_0,p_0}\Big|(\hat{x}-x_0)\right) \quad (2.9)$$

where $B(x(t), p(t))$ denotes the classical analogue of the operator. Use of this form leads to the following FBSD expression for

the time correlation function:

$$C_{AB}(t) = (2\pi\hbar)^{-1}\int dx_0 \int dp_0\, B(x_t, p_t) \times \left[\frac{3}{2}\langle g_{x_0,p_0}|\hat{\rho}_0\hat{A}|g_{x_0,p_0}\rangle - 2\gamma\langle g_{x_0,p_0}|(\hat{x}-x_0)\hat{\rho}_0\hat{A}(\hat{x}-x_0)|g_{x_0,p_0}\rangle\right] \quad (2.10)$$

The coherent state transform of the Boltzmann operator in the FBSD expression determines the weights of the initial conditions from which classical trajectories are launched. Recent work has shown that it is possible to evaluate this object using the semiclassical approximation[62] or the path integral (PI) representation of the Boltzmann operator.[37,54,57,58,60] These approaches allow inclusion of important quantum mechanical effects such as zero point energy and quantum dispersion. These effects, which are faithfully captured by PI−FBSD treatments, can amount to significant corrections to the system's partition function and, in some situations, can have even greater consequences for the calculated time evolution, leading to large imaginary components[58] and spectral asymmetries,[57] significant frequency shifts,[60] or (in the case of indistinguishable particles) effects associated with Bose condensation and superfluidity.[63]

III. Quasiclassical Evolution of the Quantized Phase Space Density

Quasiclassical approximations to time correlation functions or expectation values integrate the relevant dynamical observable at the time of interest, weighted by an appropriate phase space density. The latter is derived from the corresponding quantum mechanical operator that specifies the initial statistical distribution and may be complex valued. In many cases of practical interest, the density operator describes either a pure state (typically, the ground state of the system or a Gaussian wave packet) or a thermal ensemble. Because the density operator does not require real-time propagation, it is desirable and often possible with modest computational effort to calculate its phase space transform by accurate quantum mechanical methods, taking into account zero point energy and other quantization effects.

The benefits of a quasiclassical or forward−backward semiclassical treatment derive precisely from the possibility to accurately include quantum mechanical effects in the phase space function that determines the weights of the classical trajectories. At the same time, the combination of a quantum mechanical treatment of the initial condition with a subsequent classical propagation is inconsistent. Its most obvious shortcoming is the suspected loss of stationarity of the phase space distribution and possible violations of the detailed balance condition at finite temperature.

The particular FBSD expression under consideration, eq 2.10, takes the form of a phase space average,

$$C_{AB}(t) = (2\pi\hbar)^{-1}\int dx_0 \int dp_0\, \mathscr{P}_A(x_0, p_0)B(x_t, p_t) \quad (2.11)$$

where the phase space "density" $\mathscr{P}_A$ is a complex valued function given by the expression

$$\mathscr{P}_A(x_0, p_0) = \frac{3}{2}\langle g_{x_0,p_0}|\hat{\rho}_0\hat{A}|g_{x_0,p_0}\rangle - 2\gamma\langle g_{x_0,p_0}|(\hat{x}-x_0)\hat{\rho}_0\hat{A}(\hat{x}-x_0)|g_{x_0,p_0}\rangle \quad (2.12)$$

Other quasiclassical approximations to time correlation functions also assume a similar form. For example, in the linearized approximation of the semiclassical correlation function,[61] the density is the Wigner transform of the same operator $\hat{\rho}_0\hat{A}$:

$$W_{\hat{\rho}_0\hat{A}}(x_0, p_0) = (2\pi\hbar)^{-1}\int dx e^{-ip_0x/\hbar}\left\langle x_0 + \frac{1}{2}x\middle|\hat{\rho}_0\hat{A}\middle|x_0 - \frac{1}{2}x\right\rangle \quad (2.13)$$

The first term in the phase space density entering the FBSD correlation function is proportional to the Husimi distribution (i.e., the coherent state transform) of the operator $\hat{\rho}_0\hat{A}$. This function is always positive but is much broader than the Wigner distribution for the same system. (For certain choices of the coherent state parameter γ under nonclassical conditions, the Husimi distribution is broader than the Wigner function along *both* phase space directions.) The second term in eq 2.12 adds negative components to the wings of the distribution. The combined function is considerably narrower than the Husimi density. With suitable parameters to be discussed in the next section, the FBSD phase space density of eq 2.12 appears in general similar to the Wigner distribution. It has been pointed out that the Wigner and FBSD phase space densities are related by a Taylor expansion.[40] The appealing feature of eq 2.12 is its compact expression in terms of coherent states.

Evaluating eq 2.11 at $-t$ and applying Liouville's theorem, the correlation function is rewritten in the form

$$C_{AB}(-t) = \int dx_{-t} \int dp_{-t}\, \mathscr{P}_A(x_0, p_0)B(x_{-t}, p_{-t}) \equiv \int dx_0 \int dp_0\, \mathscr{P}_A(x_t, p_t)B(x_0, p_0) \quad (2.14)$$

Taking the complex conjugate of both sides leads to the following alternative expression for eq 2.11:

$$C_{AB}(t) = \int dx \int dp_0\, \mathscr{P}_A^*(x_t, p_t)B(x_0, p_0) \quad (2.15)$$

From this it is seen that the correlation function can also be determined by evaluating the phase space density at the phase space point reached at the time of interest by a classical trajectory. If the operator $\hat{\rho}_0\hat{A}$ that determines the phase space function $\mathscr{P}_A$ commutes with the Hamiltonian generating the dynamics, the phase space density should remain stationary and the value of the integral should remain equal to its initial value. This is the case for an expectation value ($\hat{A} = 1$) when the operator $\hat{\rho}_0$ specifying the initial density describes either an eigenstate of the same Hamiltonian or a mixed state corresponding to Boltzmann statistics. The last statement is valid within a purely classical treatment, and also for a fully quantum mechanical description of the initial condition and subsequent time evolution, since the operators involved commute in the quantum mechanical or in the classical sense. However, when the initial distribution and the dynamics are treated at different levels of approximation, the phase space distribution can change with time. In an open system that can reach thermal equilibrium, any (quantized) phase space density will eventually deform to the corresponding classical distribution. These facts imply that the expectation value of a quantum mechanical operator obtained from FBSD treatments may exhibit spurious time dependence. We note that Kapral and Ciccotti have developed a mixed quantum-classical evolution scheme[64] which, while more cumbersome and expensive, rigorously satisfies the long-time properties described above.[65]

The severity of this apparent flaw of quasiclassical approximations depends on the particular system under consideration as well as the value of the coherent state parameter γ. The latter defines the properties of the Gaussian functions. When

$\gamma \rightarrow \infty$, these functions become position eigenstates, while for $\gamma \rightarrow 0$ they reduce to momentum eigenstates. Thus γ can be viewed as an interpolation parameter between the position and momentum representations of the semiclassical propagator.[66] As the semiclassical propagator is, in general, not equally accurate in the two different representations, the accuracy of the results obtained is dependent upon γ.

The influence of γ, the coherent state parameter, upon the accuracy of semiclassical calculations has been previously examined by several groups,[14,67,68] although never specifically in reference to FBSD. In general it was found that there is a relatively large range of values of γ over which the results are accurate. This range is usually concentrated around the point where the ratio γ/γ_ω is close to one, where γ_ω is defined as $\gamma_\omega = m\omega/2\hbar$, ω being the harmonic frequency obtained from the second derivative of the potential energy function at some reference geometry for the system being studied or, more generally, the frequency that best characterizes the dynamics. It was also observed that the convergence properties of the calculation, although not its accuracy, get worse as the ratio is increased.[67]

IV. Detailed Balance

For the accurate prediction of observables, such as spectra or relaxation rates, it is essential that correlation functions obey detailed balance, i.e.,

$$G(-\omega) = e^{-\beta\omega} G(\omega) \tag{2.16}$$

where $G(\omega)$ is defined as the Fourier transform of the correlation function,

$$G(\omega) = \frac{1}{2\pi}\int_{-\infty}^{\infty} C(t) e^{i\omega t}\, \mathrm{d}t \tag{2.17}$$

By separating the correlation function into its real and imaginary parts

$$C(t) = C^{\mathrm{R}}(t) + iC^{\mathrm{I}}(t) \tag{2.18}$$

$G(\omega)$ can be split into two components,

$$G_{\mathrm{s}}(\omega) = \frac{1}{2\pi}\int_{-\infty}^{\infty} C^{\mathrm{R}}(t)\cos\,\omega t\, \mathrm{d}t \tag{2.19}$$

$$G_{\mathrm{a}}(\omega) = \frac{1}{2\pi}\int_{-\infty}^{\infty} C^{\mathrm{I}}(t)\sin\,\omega t\, \mathrm{d}t \tag{2.20}$$

so that

$$G(\omega) = G_{\mathrm{s}}(\omega) + G_{\mathrm{a}}(\omega) \tag{2.21}$$

Since $C^{\mathrm{R}}(t)$ and $C^{\mathrm{I}}(t)$ are symmetric and antisymmetric functions of t, respectively, $G_{\mathrm{s}}(\omega)$ and $G_{\mathrm{a}}(\omega)$ are both real and are symmetric and antisymmetric functions of ω. The detailed balance condition shows that $G_{\mathrm{s}}(\omega)$ and $G_{\mathrm{a}}(\omega)$ are not independent of each other but are connected by the relation[69−71]

$$G_{\mathrm{a}}(\omega) = \tanh\left(\frac{1}{2}\beta\omega\hbar\right) G_{\mathrm{s}}(\omega) \tag{2.22}$$

This implies that $C^{\mathrm{R}}(t)$ and $C^{\mathrm{I}}(t)$ are also related:[71]

$$C^{\mathrm{I}}(t) = -\tan\left(\frac{\beta\hbar}{2}\frac{d}{\mathrm{d}t}\right) C^{\mathrm{R}}(t) \tag{2.23}$$

In situations where the FBSD correlation function is very accurate, it will obviously obey detailed balance. However, since the FBSD result is in most cases an approximation, it is not clear a priori whether the detailed balance relation will be satisfied, i.e., whether the errors introduced by the FBSD approximation affect the real and imaginary parts of the correlation function equally.

To test if this detailed balance holds for the FBSD correlation function we define two new quantities

$$\tilde{C}^{\mathrm{R}}(t) = \frac{1}{2\pi}\int_{-\infty}^{\infty} \frac{G_{\mathrm{a}}(\omega)\cos\,\omega t}{\tanh(\beta\omega\hbar/2)}\, \mathrm{d}\omega \tag{2.24}$$

and

$$\tilde{C}^{\mathrm{I}}(t) = \frac{1}{2\pi}\int_{-\infty}^{\infty} \sin\,\omega t\, G_{\mathrm{s}}(\omega)\, \tanh\,(\beta\omega\hbar/2)\, \mathrm{d}\omega \tag{2.25}$$

These functions are obtained by combining eq 2.22 with eqs 2.20 and 2.21. If detailed balance is obeyed, one should have

$$\tilde{C}^{\mathrm{R}}(t) = C^{\mathrm{R}}(t), \quad \tilde{C}^{\mathrm{I}}(t) = C^{\mathrm{I}}(t) \tag{2.26}$$

for all values of t. Therefore by examining if these equalities hold we can assess whether the real and imaginary parts of the FBSD correlation function contain the same information, i.e, whether detailed balance is obeyed.

V. Model Studies

In this section we investigate the issues discussed in the previous section on model systems. Numerical calculations are presented on a one-dimensional anharmonic oscillator with a potential given by the form

$$V(x) = \frac{1}{2}m\omega^2 x^2 - 0.1x^3 + 0.1x^4 \tag{2.27}$$

with $m = 1$ and $\omega = \sqrt{2}$, and also on a condensed phase model employing the same anharmonic oscillator coupled to a 20-dimensional harmonic bath,

$$\hat{H} = \frac{\hat{p}^2}{2m} + V(\hat{x}) + \sum_{k=1}^{20}\left[\frac{\hat{p}_k^2}{2m} + \frac{1}{2}m\omega_k^2\left(\hat{q}_k - \frac{c_k\hat{x}}{m\omega_k^2}\right)^2\right] \tag{2.28}$$

The one-dimensional system in eq 2.27 was considered in earlier work by our group.[29,37] It represents a particularly challenging system for FBSD, as the strong potential anharmonicity introduces sizable quantum interference effects to the dynamics. The system-bath Hamiltonian in eq 2.28 is designed as a model for condensed phase processes. The frequencies and coupling constants of the bath are distributed according to an Ohmic spectral density[72] with $\omega_c = 4\omega$. Although the 20 degrees of freedom of the bath are not enough to provide a true dissipative environment, the observed dynamics resemble those in an environment with a continuous spectral density over several periods, certainly long enough for the present purposes.

We use an equilibrium initial condition corresponding to the Boltzmann operator for these model systems and report numerical calculations of the following quantities: (a) the time evolution of the quantized FBSD phase space density, (b) the expectation value of $\hat{x}^2$ (corresponding to the choice $\hat{A} = 1$, $\hat{B} = \hat{x}^2$), (c) the position correlation function (corresponding to the choice $\hat{A} = \hat{B} = \hat{x}$), and (d) eq 2.26 assessing the validity of the detailed balance condition.

As discussed above, the first two of these quantities should remain stationary under propagation, and thus any deviations observed below arise from the quasiclassical evolution of a quantized distribution in the FBSD formulation. In the case of the one-dimensional model, results free of statistical error are obtained for this one-dimensional system by using an expansion in terms of the system's eigenstates to evaluate the relevant matrix elements of the Boltzmann operator, $e^{-\beta\hat{H}}/Z$ (where $\beta = 1/k_B T$ and Z is the canonical partition function). The Schrödinger equation for this system was solved using the sinc-DVR method.[73] The calculations on the system-bath Hamiltonian were performed using the PI−FBSD methodolology.[37,57,60] At the lowest temperature considered, the PI−FBSD calculation employed six path integral beads.

(a) High Temperature. At high temperatures the Trotter splitting of the Boltzmann operator,

$$e^{-\beta\hat{H}} \approx e^{-\beta\hat{p}^2/4m} e^{-\beta\hat{V}} e^{-\beta\hat{p}^2/4m} \tag{2.29}$$

may be used to bring the matrix elements into the form of an integral. It is useful to consider the off-diagonal coherent state matrix element of the Boltzmann operator. The first term entering the FBSD expression, eq 2.10 becomes

$$\langle g_{x_0,p_1}|e^{-\beta\hat{H}}|g_{x_0,p_2}\rangle$$

$$\approx \sqrt{\frac{2\gamma}{\pi}}\frac{m}{m+\hbar^2\beta\gamma}\exp\left(-\frac{\beta/4}{m+\hbar^2\beta\gamma}(p_1^2+p_2^2)\right) \tag{2.30}$$

$$\times \int \mathrm{d}x \exp\left[-\frac{m}{m+\hbar^2\beta\gamma}\left(2\gamma(x-x_0)^2 + \frac{i}{\hbar}(p_1-p_2)(x-x_0)\right) - \beta V(x)\right]$$

At sufficiently high temperature, the potential factor in the integrand of the above expression varies very slowly compared to the Gaussian factor. As a result, the integral can be approximated via the steepest descent method, giving in the $\beta \to 0$ limit

$$\langle g_{x_0,p_1}|e^{-\beta\hat{H}}|g_{x_0,p_2}\rangle \approx \exp\left[-\frac{\beta}{4m}(p_1^2+p_2^2) - \frac{1}{8\hbar^2\gamma}(p_1-p_2)^2 - \beta V\left(x_0+\frac{i}{\hbar}\cdot\frac{p_1-p_2}{4\gamma}\right)\right] \tag{2.31}$$

and setting $p_1 = p_2 = p_0$ one recovers the classical expression for the Boltzmann density,

$$\langle g_{x_0,p_0}|e^{-\beta\hat{H}}|g_{x_0,p_0}\rangle \underset{\beta\to 0}{\approx} \exp\left(-\frac{\beta}{2m}p_0^2 - \beta V(x_0)\right) \tag{2.32}$$

To evaluate the second term entering the FBSD expression, eq 2.10, we apply the Trotter approximation to the off-diagonal generalization of the desired matrix element:

$$\langle g_{x_0,p_1}|(\hat{x}-x_0)e^{-\beta\hat{H}}(\hat{x}-x_0)|g_{x_0,p_2}\rangle \approx \int \mathrm{d}x \langle g_{x_0,p_1}|(\hat{x}-x_0)e^{-\beta\hat{p}^2/4m}|x\rangle e^{-\beta V(x)}\langle x|e^{-\beta\hat{p}^2/4m}(\hat{x}-x_0)|g_{x_0,p_2}\rangle \tag{2.33}$$

Using the relation

$$\langle x|e^{-\beta\hat{p}^2/4m}(\hat{x}-x_0)|g_{x_0,p_0}\rangle = -i\hbar\frac{\partial}{\partial p_0}\langle x|e^{-\beta\hat{p}^2/4m}|g_{x_0,p_0}\rangle \tag{2.34}$$

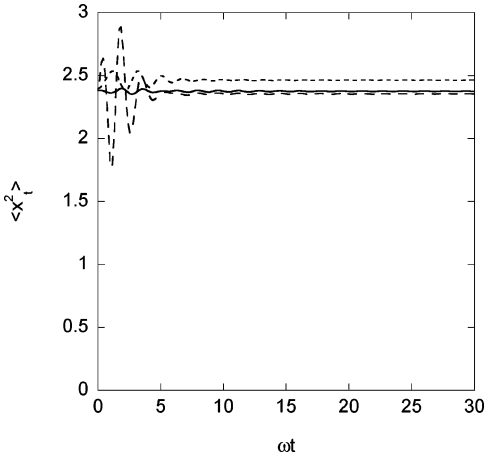

Figure 1. Expectation value of $\hat{x}^2$, eq 2.27, for the one-dimensional anharmonic oscillator at the temperature $\hbar\omega\beta = \sqrt{2}/10$. Solid line: γ/γ_ω, Short dashed line: $\gamma/\gamma_\omega = 1/8$, Long dashed line: $\gamma/\gamma_\omega = 8$.

this matrix element becomes

$$\langle g_{x_0,p_1}|(\hat{x}-x_0)e^{-\beta\hat{H}}(\hat{x}-x_0)|g_{x_0,p_2}\rangle = \hbar^2\frac{\partial^2}{\partial p_1 \partial p_2}\int \mathrm{d}x \langle g_{x_0,p_1}|e^{-\beta\hat{p}^2/4m}|x\rangle e^{-\beta V(x)}\langle x|e^{-\beta\hat{p}^2/4m}|g_{x_0,p_2}\rangle \tag{2.35}$$

Using eq 2.31 and substituting $p_1 = p_2 = p_0$ we find at high temperature

$$\langle g_{x_0,p_0}|(\hat{x}-x_0)e^{-\beta\hat{H}}(\hat{x}-x_0)|g_{x_0,p_0}\rangle \underset{\beta\to 0}{\approx} \frac{1}{4\gamma}\exp\left(-\frac{\beta}{2m}p_0^2 - \beta V(x_0)\right) \tag{2.36}$$

Substituting eqs 2.31 and 2.36 into the original FBSD expression, eq 2.12, we obtain

$$Z\,\mathscr{P}_A(x_0,p_0) \underset{\beta\to 0}{\approx} \left(\frac{3}{2}-\frac{2\gamma}{4\gamma}\right)\exp\left(-\frac{\beta}{2m}p_0^2 - \beta V(x_0)\right) \underset{\beta\to 0}{\approx} \exp\left(-\frac{\beta}{2m}p_0^2 - \beta V(x_0)\right) \tag{2.37}$$

Note that the agreement with the classical result comes from cancellation between the first and the second terms in the FBSD density.

From the above it is seen that the coherent state factor entering the FBSD expression for an expectation value reduces to the classical Boltzmann factor in the high-temperature limit. This fact implies that the FBSD formulation for the time-dependence of an expectation value reproduces in that limit the classical mechanical result,

$$\langle B(t)\rangle_{\mathrm{cl}} = Z_{\mathrm{cl}}^{-1}\int \mathrm{d}x_0 \int \mathrm{d}p_0\, e^{-\beta H(x_0,p_0)} B(x_t,p_t) \tag{2.38}$$

where Z_{cl} is the classical partition function. This conclusion applies to FBSD correlation functions as well, as long as the form of the operator $\hat{A}$ is such that the steepest descent approximation to the integral of eq 2.30 remains valid. (This condition is satisfied for linear operators. For arbitrary operators the steepest descent condition is valid for sufficiently large γ, in which case the Gaussian factor in the integrand is sharply peaked.) Under these conditions the FBSD correlation function

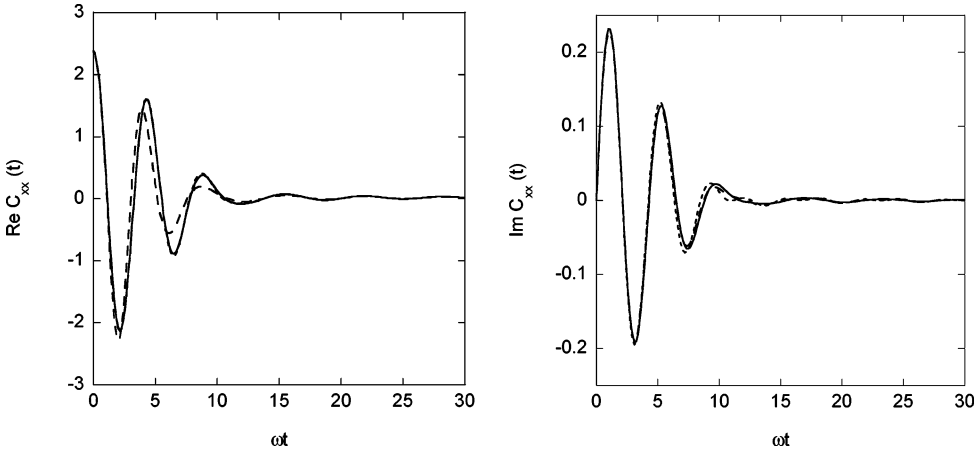

Figure 2. Dependence of the correlation function for the one-dimensional anharmonic oscillator given in eq 2.27 on the value of the coherent state parameter at $\hbar\omega\beta = \sqrt{2}/10$. Solid line: $\gamma/\gamma_\omega = 1$. Short dashed line: $\gamma/\gamma_\omega = 8$. Long dashed line: $\gamma/\gamma_\omega = 1/8$.

reduces to the classical form

$$C_{\mathrm{cl}}(t) = Z_{\mathrm{cl}}^{-1} \int \mathrm{d}x_0 \int \mathrm{d}p_0\, e^{-\beta H(x_0,p_0)} A(x_0, p_0) B(x_t, p_t) \quad (2.39)$$

The FBSD methodology becomes exact in the case of a harmonic oscillator, provided an accurate description of the density is used. In this case one recovers the quantum mechanical result for the position correlation function,

$$C_{xx}(t) \propto \coth\left(\frac{1}{2}\hbar\omega\beta\right)\cos\omega t + i \sin\omega t \quad (2.40)$$

The Taylor series expansion of this function through first order in $\hbar\omega\beta$ is

$$C_{xx}(t) \approx \left(\frac{2}{\hbar\omega\beta} + \frac{2}{3}\hbar\omega\beta\right)\cos\omega t + i \sin\omega t \quad (2.41)$$

In the high temperature limit, the above expression reduces to the classical result. One observes that the lowest order quantum correction (the term of order β) to the real part of the correlation function vanishes with increasing temperature faster than the imaginary part of the correlation function. This simple model shows that at moderately high temperatures the correlation function may have a non-negligible imaginary part, even though its real part may be well reproduced by a classical calculation.

Figure 1 shows the expectation value of $\hat{x}^2$ obtained by the FBSD methodology for the anharmonic model described by eq 2.27. Only very small fluctuations with time are observed when $\gamma/\gamma_\omega = 1$. When γ/γ_ω is changed above and below the optimal value by factors of 8, much more substantial fluctuations occur, although the asymptotic values are still rather close to each other. As shown in ref 37, the FBSD approximation to the position correlation function is essentially exact at temperatures that correspond to $\hbar\omega\beta \leq \sqrt{2}/10$. Even though the dynamics are nearly classical at this temperature, the imaginary part of the correlation function is non-negligible, with a maximum value approximately 10% of the maximum value of the real part. The weak dependence of the position correlation function on γ is shown in Figure 2, where the coherent state parameter is changed above and below the optimal value by factors of 8. The sensitivity of the results to the coherent state parameter is reduced even further in the system-bath model (but we do not show these results). Also, because the FBSD results are essentially exact at this temperature, the detailed balance condition is implicitly obeyed, and we do not examine this issue here.

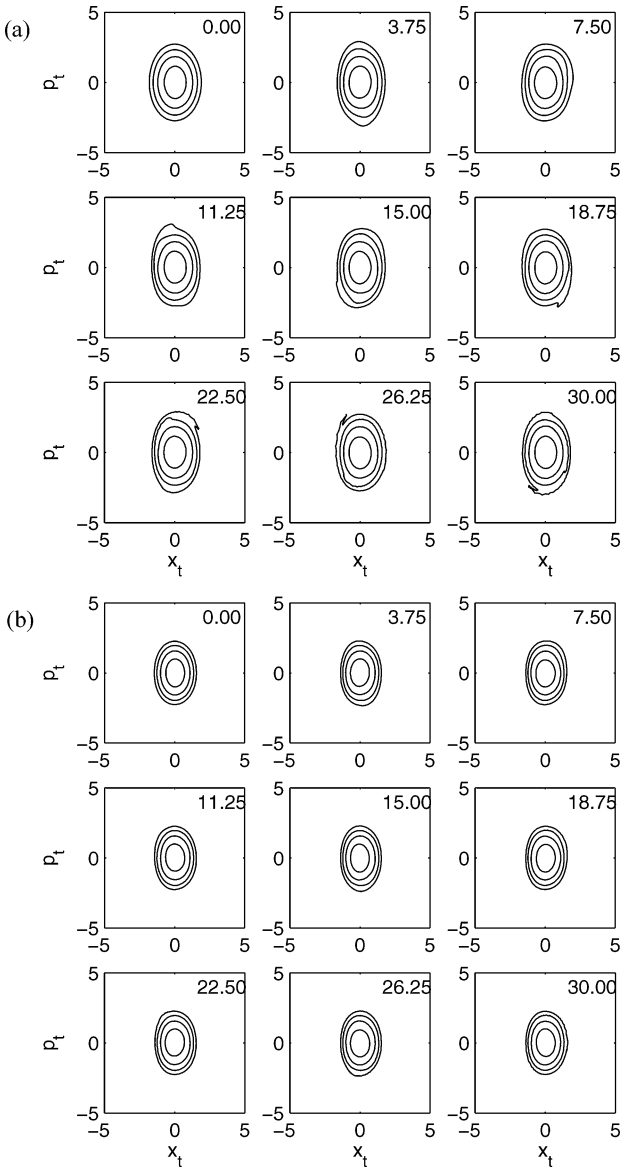

Figure 3. Contour plots of the phase space functions entering the FBSD correlation function for the anharmonic oscillator of eq 2.27 at various times. The coherent state parameter has the "optimal" value $\gamma/\gamma_\omega = 1$. The temperature is $\hbar\omega\beta = 3\sqrt{2}$. (a) The Husimi function alone (first term in eq 2.12). (b) The entire FBSD distribution given in eq 2.12. Contours are plotted at 64%, 32%, 16%, and 8% of the maximum amplitude. The time is indicated in the top right corner in units of ω^{-1}.

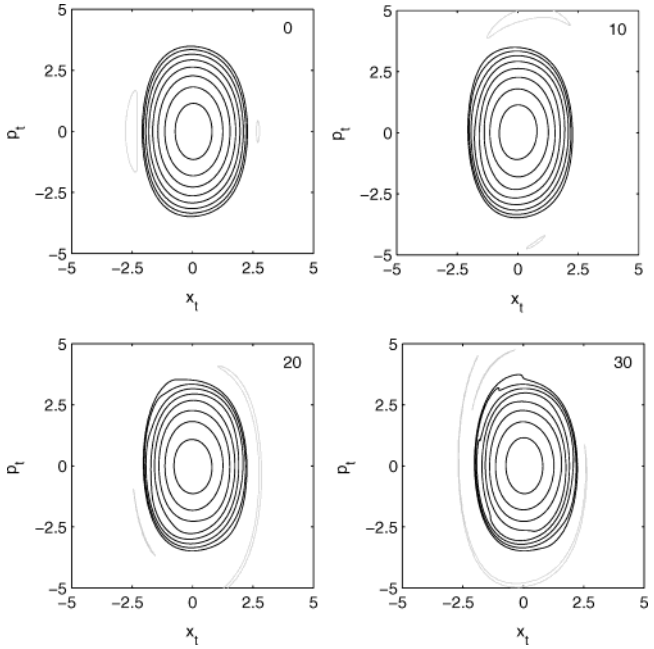

Figure 4. More detailed presentation of Figure 3b. Contours are plotted at 64, 32, 16, 8, 4, 2, 1, and 0.5% of the maximum amplitude. Negative contours are colored gray. The time in units of ω^{-1} is shown in the top right-hand corner.

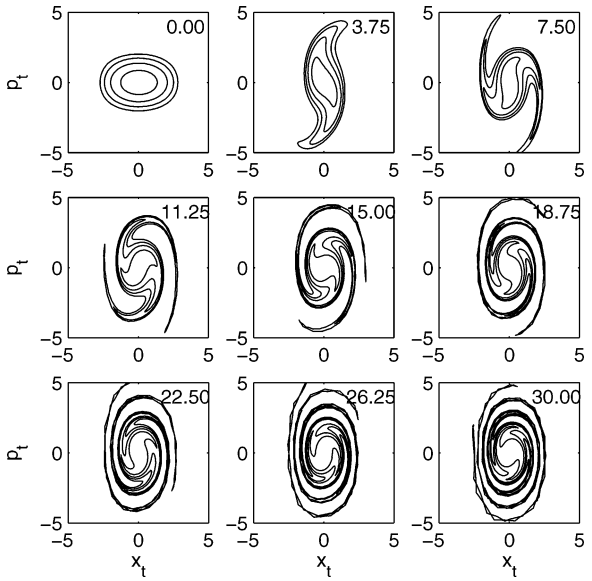

Figure 5. Contour plot of the function defined in eq 2.12 calculated using $\gamma/\gamma_\omega = 1/8$ for the temperature $\hbar\omega\beta = 3\sqrt{2}$. Contours are plotted at 64%, 32%, 16%, and 8% of the maximum amplitude. The time is indicated in the top right corner in units of ω^{-1}.

(b) Low Temperature. As the temperature is lowered, the phase space function in eq 2.15 begins to differ substantially from the classical Boltzmann density. The evolution of the phase space density function depends on the value of the coherent state parameter. This behavior is evident from the harmonic oscillator model. At zero temperature, for example, where $\hat{\rho}_0 = |\Phi_0\rangle\langle\Phi_0|$, the phase space function entering the FBSD expression is found to be

$$\mathscr{P}_{A=1}(x_t, p_t) = \frac{2\sqrt{\alpha\gamma}}{\alpha+\gamma}\exp\left(-\frac{2\alpha\gamma}{\alpha+\gamma}x_t^2 - \frac{1}{2\hbar^2(\alpha+\gamma)}p_t^2\right)\times \left[\frac{3}{2} - \frac{2\gamma}{(\alpha+\gamma)^2}\left(a^2x_t^2 + \frac{1}{4\hbar^2}p_t^2\right)\right] \quad (2.42)$$

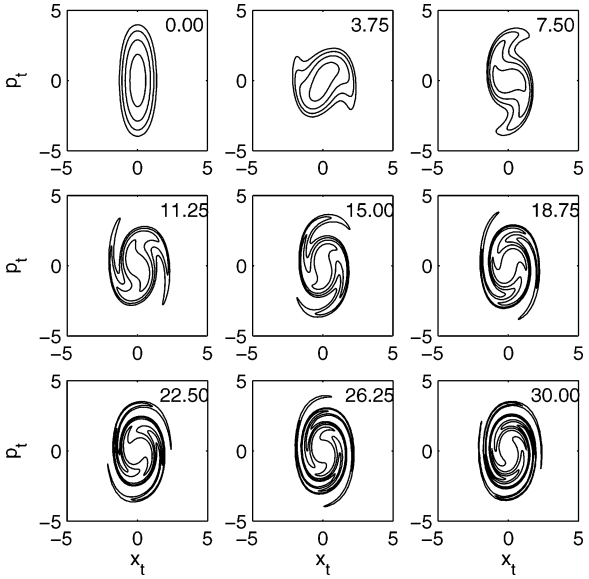

Figure 6. Contour plot of the function defined in eq 2.12 calculated using $\gamma/\gamma_\omega = 8$ for the temperature $\hbar\omega\beta = 3\sqrt{2}$. Contours are plotted at 64%, 32%, 16%, and 8% of the maximum amplitude. The time is indicated in the top right corner in units of ω^{-1}.

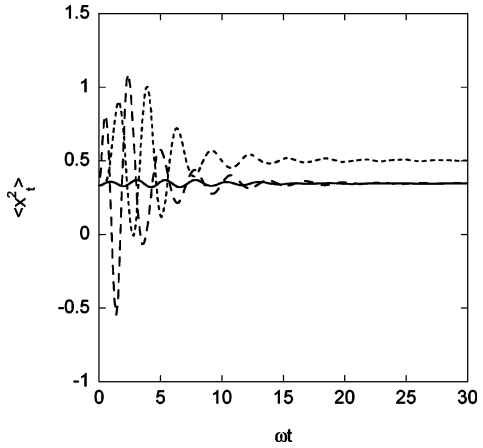

Figure 7. Expectation value of $\hat{x}^2$ for the one-dimensional anharmonic oscillator at the temperature $\hbar\omega\beta = 3\sqrt{2}$. Solid line: $\gamma/\gamma_\omega = 1$. Short dashed line: $\gamma/\gamma_\omega = 8$. Long dashed line: $\gamma/\gamma_\omega = 1/8$.

where $\alpha = m\omega/2\hbar$. This function generally rotates as the coordinates x_t, p_t follow a classical trajectory. (We note that despite this spurious evolution the expectation value of linear or quadratic operators is conserved for this system.) However, if $\gamma = \alpha$, eq 2.42 becomes

$$\mathscr{P}_{A=1}(x_t, p_t) = \exp\left(-\alpha x_t^2 - \frac{1}{4\hbar 2\alpha}p_t^2\right)\left[\frac{3}{2} - \frac{1}{2}\left(\alpha x_t^2 + \frac{1}{4\hbar 2\alpha}p_t^2\right)\right] \quad (2.43)$$

By virtue of energy conservation, the particular combination of phase space coordinates entering the above expression is preserved, and thus the density remains stationary in this case.

Similar trends are observed in the case of the one-dimensional anharmonic oscillator. In this case, the phase space density tends to develop a spiral pattern over time, as seen in Figures 3−6. The deformation is minimal for the choice $\gamma = m\omega/2\hbar$, for which the FBSD density appears nearly invariant (Figures 3b and 4), but quite pronounced when the coherent state parameter differs substantially from the above "optimal" choice (Figures 5 and 6). The role of the negative term in the FBSD density, eq

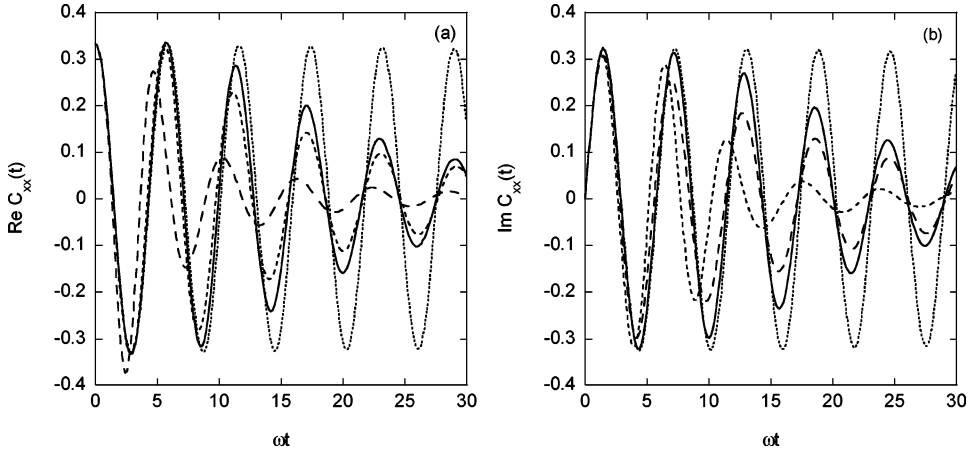

Figure 8. Dependence of the real (a) and imaginary (b) parts of the correlation function for the one-dimensional anharmonic oscillator given in eq 2.27 on the value of the coherent state parameter at $\hbar\omega\beta = 3\sqrt{2}$. Solid line: $\gamma/\gamma_\omega = 1$. Short dashed line: $\gamma/\gamma_\omega = 8$. Long dashed line: $\gamma/\gamma_\omega = 1/8$. Dotted Line: exact results.

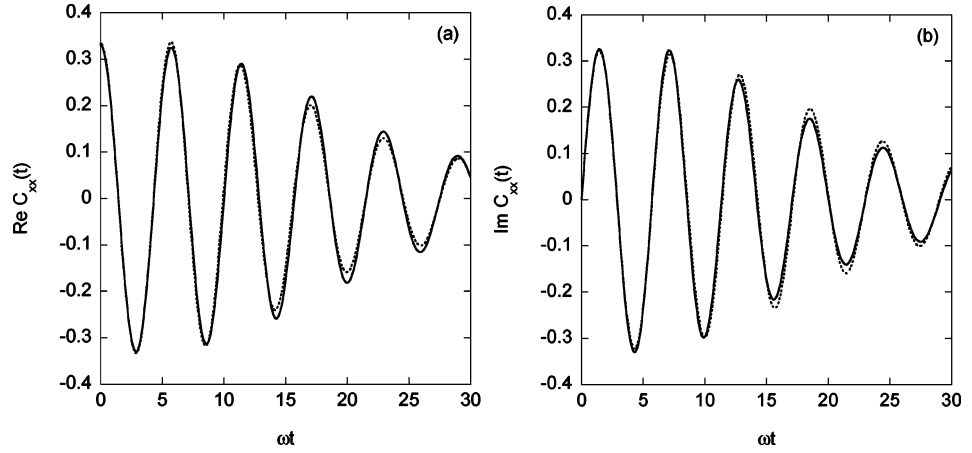

Figure 9. Real (a) and imaginary (b) parts of the position autocorrelation function for the one-dimensional anharmonic oscillator given in eq 2.27 for $\hbar\omega\beta = 3\sqrt{2}$. Dashed line: FBSD results. Solid line: results obtained from applying the detailed balance transformation defined in eqs 2.24 and 2.25.

2.12, is seen from Figures 3 and 4. Although the negative regions of the combined function are too narrow to be discerned on the contour plot of Figure 3b, the total FBSD density is substantially narrower than the Husimi distribution shown in Figure 3a. It is seen that the broader positive Husimi distribution (Figure 3a) develops small spiral wings even with the optimal choice of the coherent state parameter.

Figure 7 shows the expectation value of $\hat{x}^2$ for the same one-dimensional system. The observed fluctuations of this quantity arise from the mild evolution of the FBSD density, which occurs mostly at the wings of that function where $\hat{x}^2$ is particularly sensitive. It is interesting that the fluctuations diminish in amplitude as the time progresses and the expectation value settles to a practically constant value after three or so periods of motion. This is a consequence of the extensive fragmentation of the wings of the FBSD density at longer times, which leads to considerable cancellation.

The dependence of the FBSD results for the time correlation function on the coherent state parameter is shown in Figure 8. In contrast to the high temperature results, a much larger dependence on the value of γ/γ_ω is observed. This is not surprising, considering the degree of non-stationarity that is displayed in Figures 6 and 7. It also shows that more care must be taken in choosing the value of γ/γ_ω when the initial conditions are strongly quantum mechanical. However, it should be noted that the results obtained with $\gamma/\gamma_\omega = 2$ and $\gamma/\gamma_\omega = 4$ (not shown) are almost indistinguishable from those with $\gamma/\gamma_\omega = 1$, showing that as long as $\gamma/\gamma_\omega > 1$ there is a reasonably wide range of values of γ/γ_ω for which the FBSD calculations are stable and accurate (within the confines of the FBSD approximation).

Figures 9a and 9b show the detailed balance comparison outlined in eqs 2.24 and 2.25 for the anharmonic one-dimensional system defined in eq 2.27 calculated using the FBSD position correlation function at the lowest temperature $\hbar\omega\beta = 3\sqrt{2}$. The detailed balance relationship is satisfied at all times within the numerical accuracy of the calculation and shows that even though the FBSD approximation is breaking down, the correct relationship between the real and imaginary parts of the FBSD correlation function is maintained. This observation is in contrast to the result obtained recently by Shi and Geva,[74] who found that the detailed balance relation is not satisfied exactly for the Wigner quasiclassical approximation to the correlation function implemented within a local harmonic approximation to the Boltzmann density.

Results for the time correlation function of the system-bath Hamiltonian given in eq 2.28 are shown in Figure 10. As with the one-dimensional example, if the value of γ/γ_ω is significantly less than unity the results are qualitatively incorrect. However in this case, in contrast to the results shown in Figure 8, as γ/γ_ω begins to increase the sensitivity of the results to this parameter is, by comparison, greatly reduced.

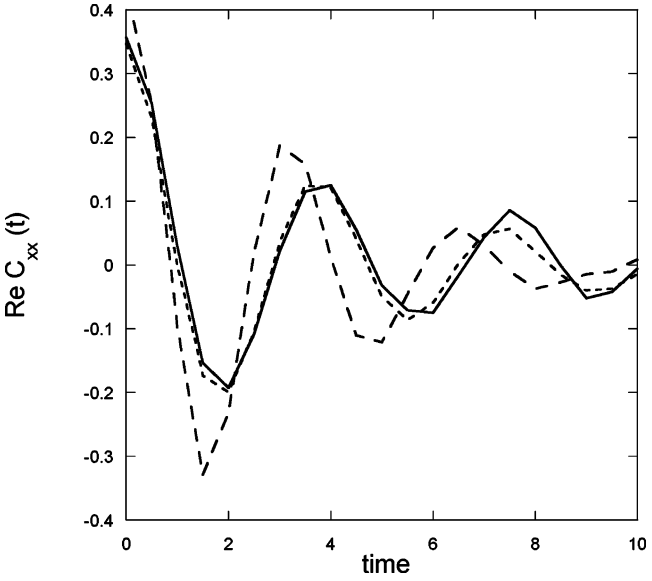

Figure 10. Comparison of the dependence of the correlation function upon γ/γ_ω for the system-bath model given in eq 2.28 at the temperature $\hbar\omega\beta = 3\sqrt{2}$. Solid line: $\gamma/\gamma_\omega = 1$. Short dashed line: $\gamma/\gamma_\omega = 8$. Long dashed line: $\gamma/\gamma_\omega = 1/8$.

The choice of which value of γ/γ_ω to use for a condensed phase calculation is clarified somewhat by this analysis. Putting aside coordinate system considerations, which will be system specific, it seems that using a value slightly larger than that suggested by the pair potential is a reasonably safe choice, given the smaller sensitivity of the results for larger than optimal values of the coherent state parameter. One should also note that the highest frequency present in the system will often be larger than that predicted from the pair potential in the condensed phase because of solvent caging type effects, and this is another reason to opt for slightly larger values of γ/γ_ω. As demonstrated in Figures 1 and 7, examination of an expectation value that should remain time-independent provides an excellent practical way of checking the validity of the results.

VI. Concluding Remarks

The FBSD method shows much promise as a tool for including quantum mechanical effects into the calculation of time-dependent observables or correlation functions in the condensed phase. In this paper we have presented a detailed analysis of various important issues surrounding FBSD calculations.

First, we have shown that the method in practice obeys detailed balance. This tells us that the relationship between the real and imaginary parts of the FBSD correlation function is correct, even if the FBSD approximation itself is breaking down.

We have also investigated how the results of a FBSD calculation depend on the value of the coherent state parameter. Our analysis suggests that by using a value of the parameter slightly larger than that suggested by the pair potential is the optimum choice. This is broadly in line with the recommendation of Yamamoto and Miller,[67] whose analysis did not specifically concentrate upon FBSD. We also showed that for a simple model of the condensed phase, based upon a system-bath type Hamiltonian, the presence of the bath reduces the sensitivity of the results to the value of the coherent state parameter, suggesting that for a condensed phase calculation one does not need to put extensive efforts into choosing the value to use for the simulation.

The results generated in this paper provide a better understanding of FBSD time evolution and give us confidence to use the FBSD method to continue to explore dynamical processes in the condensed phase that exhibit significant quantum mechanical effects.

Acknowledgment. This work supported by the National Science Foundation under Award No. NSF CHE 02-12640. N.J.W. thanks Dr. Akira Nakayama for valuable discussions about performing FBSD calculations.

References and Notes

(1) Van Vleck, J. H. *Proc. Nat. Acad. Sci. U.S.A.* **1928**, *14*, 178.
(2) Morette, C. *Phys. Rev.* **1952**, *81*, 848.
(3) Miller, W. H. *Adv. Chem. Phys.* **1974**, *25*, 69.
(4) Miller, W. H. *Adv. Chem. Phys.* **1975**, *30*, 77.
(5) Herman, M. F.; Kluk, E. *Chem. Phys.* **1984**, *91*, 27.
(6) Kluk, E.; Herman, M. F.; Davis, H. L. *J. Chem. Phys.* **1986**, *84*, 326.
(7) Heller, E. J.; Reimers, J. R.; Drolshagen, G. *Phys. Rev. A* **1987**, *36*, 2613.
(8) Child, M. S. *Semiclassical mechanics with molecular applications*; Clarendon: Oxford, 1991.
(9) Heller, E. J. *J. Chem. Phys.* **1991**, *94*, 2723.
(10) Tomsovic, S.; Heller, E. J. *Phys. Rev. Lett.* **1991**, *67*, 664.
(11) Sepulveda, M. A.; Tomsovic, S.; Heller, E. J. *Phys. Rev. Lett.* **1992**, *69*, 402.
(12) Campolieti, G.; Brumer, P. *Phys. Rev. A* **1994**, *50*, 997.
(13) Kay, K. G. *J. Chem. Phys.* **1994**, *100*, 4377.
(14) Kay, K. G. *J. Chem. Phys.* **1994**, *100*, 4432.
(15) Sepulveda, M. A.; Grossmann, F. *Adv. Chem. Phys.* **1996**, *XCVI*, 191.
(16) Walton, A. G. R.; Manolopoulos, D. E. *Mol. Phys.* **1996**, *84*, 961.
(17) Cao, J.; Voth, G. A. *J. Chem. Phys.* **1996**, *104*, 273.
(18) Brewer, M. L.; Hulme, J. S.; Manolopoulos, D. E. *J. Chem. Phys.* **1997**, *106*, 4832.
(19) Garashchuk, S.; Grossmann, F.; Tannor, D. *J. Chem. Soc., Faraday Trans.* **1997**, *93*, 781.
(20) Kay, K. *J. Chem. Phys.* **1997**, *107*, 2313.
(21) Sun, X.; Miller, W. H. *J. Chem. Phys.* **1997**, *106*, 916.
(22) Wang, H.; Sun, X.; Miller, W. H. *J. Chem. Phys.* **1998**, *108*, 9726.
(23) Hernandez, R.; Voth, G. A. *Chem. Phys.* **1998**, *233*, 243.
(24) Sun, X.; Wang, H.; Miller, W. H. *J. Chem. Phys.* **1998**, *109*, 4190.
(25) Makri, N.; Thompson, K. *Chem. Phys. Lett.* **1998**, *291*, 101.
(26) Miller, W. H. *Faraday Discuss.* **1998**, *110*, 1.
(27) Thompson, K.; Makri, N. *J. Chem. Phys.* **1999**, *110*, 1343.
(28) Thompson, K.; Makri, N. *Phys. Rev. E* **1999**, *59*, R4729.
(29) Shao, J.; Makri, N. *J. Phys. Chem. A* **1999**, *103*, 7753.
(30) Shao, J.; Makri, N. *J. Phys. Chem. A* **1999**, *103*, 9479.
(31) Grossmann, F. *Phys. Rev. A* **1999**, *60*, 1791.
(32) Sun, X.; Miller, W. H. *J. Chem. Phys.* **1999**, *110*, 6635.
(33) Wang, H.; Thoss, M.; Miller, W. H. *J. Chem. Phys.* **2000**, *112*, 47.
(34) Garashchuk, S.; Light, J. C. *J. Chem. Phys.* **2000**, *113*, 9390.
(35) McQuarrie, B. R.; Brumer, P. *Chem. Phys. Lett.* **2000**, *319*, 27.
(36) Shao, J.; Makri, N. *J. Chem. Phys.* **2000**, *113*, 3681.
(37) Jezek, E.; Makri, N. *J. Phys. Chem.* **2001**, *105*, 2851.
(38) Makri, N. Forward−backward semiclassical dynamics. In *Fluctuating paths and fields*; Janke, W., Pelster, A., Schmidt, H.-J., Bachmann, M., Eds.; World Scientific: Singapore, 2001.
(39) Wang, H.; Thoss, M.; Sorge, K. L.; Gelabert, R.; Gimenez, X.; Miller, W. H. *J. Chem. Phys.* **2001**, *114*, 2562.
(40) Thoss, M.; Wang, H.; Miller, W. H. *J. Chem. Phys.* **2001**, *114*, 9220.
(41) Wilkie, J.; Brumer, P. *Phys. Rev. A* **2001**, *61*, 064101.
(42) Zhao, Y.; Makri, N. *Chem. Phys.* **2002**, *280*, 135.
(43) Sun, X.; Miller, W. H. *J. Chem. Phys.* **1998**, *108*, 8870.
(44) Batista, V. S.; Zanni, M. T.; Greenblatt, J.; Neumark, D. M.; Miller, W. H. *J. Chem. Phys.* **1999**, *110*, 3736.
(45) Zanni, M. T.; Batista, V. S.; Greenblatt, J.; Miller, W. H.; Neumark, D. M. *J. Chem. Phys.* **1999**, *110*, 3748.
(46) Skinner, D. E.; Miller, W. H. *J. Chem. Phys.* **1999**, *111*, 10787.
(47) Thoss, M.; Miller, W. H.; Stock, G. *J. Chem. Phys.* **2000**, *112*, 10282.
(48) Coronado, E. A.; Batista, V. S.; Miller, W. H. *J. Chem. Phys.* **2000**, *112*, 5566.
(49) Guallar, V.; Batista, V. S.; Miller, W. H. *J. Chem. Phys.* **2000**, *113*, 9510.
(50) Wang, H.; Manolopoulos, D. E.; Miller, W. H. *J. Chem. Phys.* **2001**, *115*, 6317.

(51) Miller, W. H. *J. Phys. Chem.* **2001**, *105*, 2942.
(52) Gelabert, R.; Giménez, X.; Thoss, M.; Wang, H.; Miller, W. H. *J. Chem. Phys.* **2001**, *114*, 2572.
(53) Ovchinnikov, M.; Apkarian, V. A.; Voth, G. A. *J. Chem. Phys.* **2001**, *114*, 7130.
(54) Yamamoto, T.; Wang, H.; Miller, W. H. *J. Chem. Phys.* **2002**, *116*, 7335.
(55) Yamamoto, T.; Miller, W. H. *J. Chem. Phys.* **2003**, *118*, 2135.
(56) Zhao, Y.; Miller, W. H. *J. Chem. Phys.* **2002**, *117*, 9605.
(57) Wright, N. J.; Makri, N. *J. Chem. Phys.* **2003**, *119*, 1634.
(58) Nakayama, A.; Makri, N. *J. Chem. Phys.* **2003**, *119*, 8592.
(59) Makri, N.; Shao, J. Semiclassical time evolution in the forward−backward stationary phase limit. In *Accurate description of low-lying electronic states and potential energy surfaces*; Hoffmann, M., Ed.; Oxford University Press: Oxford, 2002.
(60) Makri, N. *J. Phys. Chem. B* **2002**, *106*, 8390.
(61) Sun, X.; Wang, H.; Miller, W. H. *J. Chem. Phys.* **1998**, *109*, 7064.
(62) Makri, N.; Miller, W. H. *J. Chem. Phys.* **2002**, *116*, 9207.
(63) Nakayama, A.; Makri, N. *Chem. Phys.*, to be submitted.
(64) Kapral, R.; Ciccotti, G. *J. Chem. Phys.* **1999**, *110*, 8919.
(65) Nielsen, S.; Kapral, R.; Ciccotti, G. *J. Chem. Phys.* **2001**, *115*, 5805.
(66) Miller, W. H. *Mol. Phys.* **2002**, *100*, 397.
(67) Yamamoto, T.; Miller, W. H. *J. Chem. Phys.* **2003**, *118*, 2135.
(68) Zhang, S.; Pollak, E. *J. Chem. Phys.* **2003**, *119*, 11058.
(69) Egorov, S. A.; Everitt, K. F.; Skinner, J. L. *J. Phys. Chem.* **1999**, *103*, 9494.
(70) Frommhold, L. *Collision-induced adsorption in gases*; Cambridge University Press: Cambridge, 1993.
(71) Barocchi, F.; Moraldi, M.; Zoppi, M. *Phys. Rev. A* **1982**, *26*, 2168.
(72) Caldeira, A. O.; Leggett, A. J. *Physica A* **1983**, *121*, 587.
(73) Colbert, D. T.; Miller, W. H. *J. Chem. Phys.* **1992**, *96*, 1982.
(74) Shi, Q.; Geva, E. *J. Phys. Chem. A* **2003**, *107*, 9059.